SYNTHESIS AND CHARACTERIZATION OF COBALT NANOPARTICLES PREPARED BY LIQUID-PHASE REDUCTION

MARY DONNABELLE L. BALELA

UNIVERSITI SAINS MALAYSIA
2008

SYNTHESIS AND CHARACTERIZATION OF COBALT NANOPARTICLES PREPARED BY LIQUID-PHASE REDUCTION

by

MARY DONNABELLE L. BALELA

Thesis submitted in
fulfillment of the
requirements for the
Degree of Master of Science

July 2008

ACKNOWLEDGEMENTS

I would like to extend my gratitude to the following individuals and institutions for their significant contributions in making the current research work possible:

- **Dr. Zainovia Lockman**, for her constant probing, questioning, and correcting, for her unbelievable patience, for teaching me the value of research and what it takes to produce a good one.

- **Dr. Azizan Aziz**, for the conversations, debates, and arguments, for the commendable patience as well.

- **Prof. Eiichiro Matsubara and Dr. Alberto Amorsolo Jr.,** for their valuable suggestions and advices.

- **AUNSEED-Net/JICA**, for the scholarship and financial assistance.

- **Pn. Fong, Pn. Haslina, Zaini, Zul, En. Suhaimi, En. Azrul, En. Azam, En. Rashid**, for the company and assistance during experiments. Laboratory work was never dull because of these people.

- **Mr. Muthu and the staff of the Electron Microscope Laboratory, School of Biology, USM**, for the encouragements and support especially during those long months of frustrations and failures.

- **Mr. Karuna of the Crystallography Laboratory, School of Physics, USM**, for the assistance in the XRD analysis.

- **Dr. Mohd and En. Elias of SIRIM-AMREC**, for the help on the magnetic measurements.

- **Kak Na, Kak Mila, and the rest of the administrative staff of the School of Materials and Mineral Resources Engg, USM**, for their assistance on purchases and testing.

- **Ng, Chia, and Hwee Yeo**, for the help during TEM and XRD testing and for the interesting discussions in the labs.

- **Laili and Dr. Azizan Aziz**, for the abstract translation.

- **Vilay, Erfan, Tedi, Mr. Toguh, Luan, Viet, Dika, Kim, Nad, Parisha, and to all my USM friends**, for putting up with me these past two years.

- To my **family**, for their encouragement and support.

- **Eugene Clef** – for the blind faith, for being there 24/7, for keeping me sane everyday, for making my life fun, interesting, and worth living.

Most of all, to **God Almighty** for all the blessings and opportunities He bestowed on me; for the good health and for each day of being alive.

TABLE OF CONTENTS

LIST OF TABLES

LIST OF FIGURES

LIST OF ABBREVIATIONS

AFM	: Antiferromagnetic
AOT	: Bis(2-ethylhexyl) S-sodium Sulfosuccinate
CTAB	: Centrimethyl Ammonium Bromide
DDAB	: Didodecyldimethyl Ammonium Bromide
DMF	: N,N dimethylformamide
EDTA	: Ethylenediamine-N,N,N',N'-tetracetic
EDX	: Energy Dispersive X-ray Spectroscopy
EG	: Ethylene Glycol
FCC	: Face-Centered Cubic
FE-SEM	: Field Emission Scanning Electron Microscope
HCP	: Hexagonal Close-Packed
LA	: Lauric Acid
NTA	: Nitrilotriacetic Acid
OA	: Oleic Acid
PG	: Propylene Glycol
$(ph)_3P$	: Triphenylphosphine
PR_3	: Trialkylphosphine
SDS	: Sodium Dodecylsulfosuccinate
STP	: Standard Temperature and Pressure
TEM	: Transmission Electron Microscope
TGA	: Thermogravimetric Analysis
TOPO	: Trioctylphosphane Oxide
Triton X-100	: Polyoxyethylene(10) Isooctylphenyl Ether
VSM	: Vibrating Sample Magnetometer
XRD	: X-ray Diffraction

LIST OF SYMBOLS

a	: Lattice parameter
A	: Area
Ag	: Silver
Ar	: Argon
Au	: Gold
BH_4^-	: Borohydride ion
β	: Beta
Co	: Cobalt
$Co_2(CO)_8$	: Dicobalt octacarboynyl
E°	: Standard electrode potential
ε	: Epsilon
Fe	: Iron
H_2	: Hydrogen gas
$LiBEt_3H$	: Lithium hydride
MBH_4	: Metal tetraborohydrates
Mn	: Manganese
N_2H_4	: Hydrazine
$N_2H_5^+$	: Hydrazinium ion
$NaBH_4$	: Sodium borohydride
NaOH	: Sodium hydroxide
Ni	: Nickel
Pd	: Palladium
Pt	: Platinum
PVP	: Poly vinyl pyrrolidone
ρ	: Density
μ_B	: Bohr magneton
V	: Volume

SINTESIS DAN PENCIRIAN NANOPARTIKEL KOBALT MELALUI PENURUNAN FASA-CECAIR

ABSTRAK

Nanopartikel Co telah dihasilkan secara penurunan fasa-cecair menggunakan N_2H_4 dan propilena glikol tanpa sebarang agen perlindungan. Nanopartikel yang amat halus dan bulat disediakan dengan penurunan Co^{2+} menggunakan N_2H_4 dalam larutan etilena glikol berbes. Nanopartikel kelihatan diskret dan terserak dengan baik bila ditaburkan dalam etilena glikol. Walaubagaimanapun nanopartikel bergumpal ke saiz submikron bila dimendakan dari larutan. Diperhatikan juga bahawa penurunan Co^{2+} oleh N_2H_4 adalah perlahan, walaupun suhu, kepekatan N_2H_4 dan Co^{2+} tindak balas dipertingkatkan. Sebaliknya partikel Co yang lebih besar dan bersaiz seragam antara 30 nm hingga 400 nm serta berbentuk kuasi-sfera dihasilkan dalam propilena glikol dan saiz partikel dikawal dengan mengubah kepekatan prekursor dan menambah agen penukleusan $AgNO_3$, $PdCl_2$ dan H_2PtCl_6. Meningkatkan amaun prekursor, termasuk nisbah agen penukleusan $AgNO_3$ atau $PdCl_2$ menghasilkan partikel Co yang kecil. Dalam kes Pt, saiz partikel kekal dalam semua nisbah agen penukleusan H_2PtCl_6 yang dikaji. Saiz partikel Co yang paling kecil 30 – 80 nm disintesis dengan Pt. Pembelauan Sinar –X menunjukkan kedua kaedah menghasilkan campuran Co heksagonal susun-padat dan kubik berpusat muka. Sukatan magnet pada suhu bilik menunjukkan partikel Co yang disediakan dalam propilena glikol semuanya ferromagnet dengan had domain-tunggal 61 nm. Pengoksidaan termal sampel menunjukkan partikel-partikel yang dihasilkan tidak mudah teroksida dibawah 200°C kerana kewujudan lapisan bendasing pasif. Melepasi suhu ini, lapisan bendasing ini terurai dan partikel Co teroksida kepada Co_3O_4.

SYNTHESIS AND CHARACTERIZATION OF COBALT NANOPARTICLES PREPARED BY LIQUID-PHASE REDUCTION

ABSTRACT

Co nanoparticles were produced by liquid-phase reduction using N_2H_4 and propylene glycol without any protective agent. Very small, though polydispersed, spherical Co nanoparticles were prepared by Co^{2+} reduction using N_2H_4 in a basic ethylene glycol solution. The nanoparticles appeared to be discrete and well-separated when dispersed in ethylene glycol. However, they agglomerated to submicron-sized particles when precipitated from the solution. It was also inferred that the reduction of Co^{2+} by N_2H_4 was generally very slow, though the reaction was enhanced by an elevated temperature, a high N_2H_4 concentration, and a large amount of Co^{2+}. On the other hand, larger but monodispersed quasi-spherical Co particles with sizes between 30 nm to 400 nm were produced in propylene glycol and the particle size was tailored by varying the precursor concentration and by adding nucleating agents such as $AgNO_3$, $PdCl_2$, and H_2PtCl_6. Increasing the amount of precursor, as well as $AgNO_3$ or $PdCl_2$ nucleation ratios, formed smaller Co particles. In the case of samples with Pt, the particle size remained almost constant in all H_2PtCl_6 nucleation ratios explored. Even so, the smallest Co particles of 30 – 80 nm in diameters were synthesized with Pt. XRD then showed that both methods produced mixtures of HCP and FCC-Co. Room-temperature magnetic measurements revealed that the Co particles prepared in propylene glycol were all ferromagnetic with a single-domain limit of 61 nm. Thermal oxidation of the samples showed that they were not susceptible to oxidation below 200 ˚C due to the passivation of the impurity layer. Beyond this temperature, the impurity layer decomposed and the Co particles oxidized to Co_3O_4.

CHAPTER 1
INTRODUCTION

1.1 Background of the Study and Problem Statement

Nanoparticles are zero-dimensional nanostructures (Cao, 2004; Gubin et al., 2005) and are generally classified according to their composition: metal oxides, noble metals, transition metals, magnetic metals, etc. (Cao, 2004; Sergeev, 2006). Like all nanostructures, the properties of nanoparticles are dependent on their size and shape. The variation of their properties at the nanoscale is not a result of a scaling factor, but stems from different causes in different materials (Burda et al., 2005). In semiconductor, it is due to the further confinement of the electronic motion to a length scale that is comparable to or less than the length scale of the electronic motion in bulk semiconductors (Moriarty, 2001). In noble metals, it results from the strong absorption of radiation within the visible region leading to the collective oscillation of the electrons in the conduction band, called surface plasmon resonance, from the surface of one particle to another (Burda et al., 2005). In transition metals, it arises from the large surface to volume ratio resulting to high chemical activities (Toshima, 2003). And in magnetic metals, it is due to finite-size and surface effects, which become increasingly important as the particle size of the magnetic material is reduced (Batlle and Labarta, 2002).

Co is a well-known ferromagnetic material which is commonly used as an alloying element in permanent magnets (Goldman, 1999). It exists in two forms: HCP (hexagonal close-packed) and FCC (face-centered cubic). HCP is the stable phase at room temperature, whereas FCC is stable at temperatures above 450 ˚C (Dinega and Bawendi, 1999).

In nanosized, Co particles display a wide range of interesting size-dependent structural, electrical, magnetic, and catalytic properties (Puntes et al., 2001). In particular, because of their large surface area, Co nanoparticles showed high chemical reactivity, which makes them suitable for catalysis (Hyeon, 2002). Furthermore, below a critical size of 20 nm, they behave as singe-domain particles displaying quantum size effects, superparamagnetism, large magnetic anisotropies, and a maximum coercivity (Ram, 2001). Moreover, at this size range, a new metastable phase can also be formed, called ε-Co that has a complex β-Mn structure and has properties in between the HCP and FCC phases. ε-Co can be prepared by solution chemistry, particularly via organometallic route in the presence of tight binding ligands (Dinega and Bawendi, 1999; Sun and Murray, 1999). Thus, these previous studies prove that Co as a nanomaterial is an excellent and interesting system to study.

Future applications of Co nanoparticles in the fields of separation technology, information storage systems, catalysis, and biomedicine (Kodama, 1999) require the nanoparticles to be discrete, identical in size and shape, and uniform in composition and crystal structure (Cao, 2004). However, formation of nanoparticles satisfying these requirements prove to be difficult due to their high surface energy, their intrinsic magnetic properties, and the inherent limitations of the available processes. In addition, there are also concerns regarding the reproducibility of the existing methods.

By far, liquid-phase synthetic routes are the most successful in the preparation of monodispersed Co nanoparticles. Examples of liquid-phase processes

are metal salt reduction, reverse micelles, and thermal decomposition of organometallic precursor. Among these methods, direct metal salt reduction in solution is the simplest, fastest, and the least expensive, which are desirable for future attempts of large-scale production (Guo et al., 2002).

An important component of metal salt reduction processes is the protective agent. Protective agents such as surfactants that form a layer of molecular membrane around the nanoparticles and polymers that provide steric hindrance between nanoparticles are added during the reaction to inhibit particle agglomeration and to control the particle growth. However, besides posing as an additional cost to the total cost of the synthesis, they may complicate the cleaning process of the nanoparticles since they are not easy to remove by simple washing and might require secondary cleaning process, such as annealing, to decompose the protective agents covering the nanoparticles (Wu and Chen, 2003). Moreover, selection of the suitable protective agent for a particular reaction is a tedious task of trial-and-error, since the surface chemistry of the nanoparticles is complex due to their high surface energy and their tendency to accumulate surface charges. Thus, the interaction of the protective agent with the solvent and with the nanoparticles plus its properties, such as the solubility in the solvent, molecular weight, and the amount needed for stabilization, must be taken into account when choosing the right protective agent. Thus, in some cases, agglomeration of nanoparticles still occurred even in the presence of protective agents (Chou and Huang, 2001; Lee and Chen, 2006). One way to solve the problem is by the choice of a solvent that can also act as protective agent. In this way, not only the nanoparticles can be protected, but the process will be cheaper and more straightforward.

In this study, preparation of Co nanoparticles was performed using Co salt reduction technique, without adding protective agents. Polyalcohols such as ethylene glycol and propylene glycol were used as solvents and their ability to act as the dispersing agent and growth inhibitors were also evaluated based from the average particle size and size distribution of the Co nanoparticles. Therefore, the development of "protective-agent free" methods will greatly simplify the formation of cobalt nanoparticles by liquid-phase reduction.

1.2 Objectives of the Study

As mentioned, the formation of Co nanoparticles is accomplished by Co salt reduction technique without any protective agent. The objectives of this work are:

(a) to prepare uniformly sized, monodispersed, and size-tunable Co nanoparticles using a simplified Co salt reduction process.

(b) to investigate the morphology, crystal structure, magnetic properties, and oxidation behavior of the Co nanoparticles.

1.3 Project Overview

In achieving the objectives, three main experiments were conducted. The first experiment involves the reduction of Co ions in a basic ethylene glycol solution using hydrazine, N_2H_4, as reductant. The size of the Co nanoparticles were tuned by varying the reaction temperature, stirring speed, precursor concentration, and amount of N_2H_4. However, in all samples, the particle size distribution was broad with a relative standard deviation greater than 20%. Furthermore, severe agglomeration of the nanoparticles was observed after precipitation.

To obtain Co nanoparticles with narrower size distribution, a second experiment using the polyol method was explored, which was accomplished by heating an alkaline solution of propylene glycol containing Co acetate up to the boiling temperature for about two hours with reflux. Control of particle size was achieved by varying the precursor concentration and by the addition of nucleating agents. A set of experiments was also performed to study the effect of PVP k15 as protective agent on the morphology and agglomeration of the nanoparticles. Furthermore, this was also done to demonstrate how addition of protective agent can complicate the synthesis and the cleaning procedure of the nanoparticles.

Standard characterization techniques such as TEM, XRD, FE-SEM, EDX, and VSM were then performed on the synthesized Co nanoparticles.

The third experiment was conducted to study the oxidation behavior of monodispersed Co nanoparticles obtained from the second experiment. Firstly, this is important to compare the oxidation behavior of bulk Co or Co in a bar form to that of the nanoparticles and to investigate the effects of the nucleating agent and the impurity layer on the surface of the nanoparticles on their oxidation properties. Thermal oxidation of Co nanoparticles was achieved by exposing the nanoparticles in flowing oxygen gas and increasing temperature in TGA. Oxidized nanoparticles were also sent for XRD analysis to identify the phases present.

CHAPTER 2
LITERATURE REVIEW

2.1 Introduction

Nanotechnology deals with the ability to fully control the properties of nanostructured materials through their size, shape, and composition, as well as with the fabrication of reproducible complex structures from simpler systems (Eggeman et al., 2006). The development of nanotechnology is expected to proceed at several levels: materials, devices, and systems (Salata et al., 2004). Currently, the most advanced in terms of scientific knowledge and potential industrial application is the materials level (Hyeon, 2002; Salata et al., 2004).

Nanostructured materials refer to those materials whose structural elements (crystallites, clusters, or molecules) have sizes less than 100 nm at least in one dimension (Moriarty, 2001). These include nanoparticles, nanorods, nanowires, nanotubes, and thin films among others (Cao, 2004). Interest on these materials lies on their novel electrical, optical, chemical and magnetic properties that have great technological and fundamental scientific importance due to their remarkable difference from the properties of their bulk counterparts. Furthermore, by controlling their size and interactions, the fundamental properties of these materials maybe tailored (Cushing et al., 2004). Thus, it is clear that utilizing these materials fully and effectively depends on the understanding of their preparation, their general properties, and the factors that influence these properties.

As mentioned, nanoparticles are zero-dimensional nanostructured materials in which all characteristics linear dimensions are of the same order of magnitude

(Cao, 2004; Gubin et al., 2005). A special class of nanoparticles, i.e. magnetic nanoparticles, exhibit unique phenomena such as superparamagnetism, high coercivity, high saturation field, and exchanged anisotropy due to a thin layer of antiferromagnetic oxide formed around the ferromagnetic core of the nanoparticles because of their subsequent exposure to air (Tartaj et al., 2003). These phenomena are attributed to size and surface effects that dominate the behavior of magnetic particles in nanosized range (Batlle and Labarta, 2002). Typical examples are Co nanoparticles.

Therefore, in this chapter, the structural, magnetic and oxidation properties of bulk Co are described and these macroscopic properties are then compared to the reported properties of nanosized Co particles. Since monodispersed and discrete nanoparticles are required to realize their applications, the general principles for the formation of uniformly sized nanoparticles are explained and the common liquid-phase synthetic routes for Co and other magnetic nanoparticles are also described. Emphasis is given on these methods by virtue of their wide application and success in the preparation of monodispersed and high quality Co nanoparticles. Furthermore, the general effects of synthesis parameters such as temperature, precursor concentration, reductant, and protective agent on the nanoparticle size and size distribution are also discussed. Lastly, the potential applications of Co nanoparticles in separation technology, catalysis, high-density magnetic recording, and biomedicine are reviewed.

2.2 Cobalt Allotropes and their Allotropic Phase Transformations: for Bulk and Nanosized Particles

It has been known that bulk cobalt exists in two allotropes, namely: (a) hexagonal close-packed Co (HCP-Co) and (b) face-centered cubic Co (FCC-Co). Thermodynamically, HCP-Co is the stable phase below 450 ˚C, while FCC-Co forms at higher temperatures (Erbudak et al., 1997; Sato et al., 1997; Dinega and Bawendi, 1999). Accordingly, these phases are in equilibrium at about 422 – 427 ˚C (Dinega and Bawendi, 1999).

Because of the difference in crystal structure, variations in physical and magnetic properties between the two polymorphs arise. HCP-Co is slightly denser than FCC-Co, even though both phases are close-packed structures (Dinega and Bawendi, 1999). Furthermore, HCP-Co is also magnetically harder than the FCC phase due to its magnetic anisotropy and high coercivity as compared to the symmetrical and low coercivity FCC phase (Shukla et al., 2006). Thus, the highly anisotropic HCP-Co is more desirable for magnetic recording and other permanent magnet applications. On the other hand, the FCC phase is more suitable for soft magnetic applications (Dinega and Bawendi, 1999; Sun and Murray, 1999; Shukla et al., 2006). The HCP and FCC crystal structures of Co are illustrated in Fig. 2.1 (a) and (b) respectively, while the values of the crystal lattice parameter, lattice surface area, lattice volume, and calculated densities for bulk HCP and FCC-Co are summarized in Table 2.1.

The HCP$\rightarrow$FCC bulk phase transformation is reversible and weakly first order. It is also accompanied by a small change in enthalpy (ΔH) of about 440

kJ/mol and in volume ($\Delta V/V$) which is approximately equal to 0.0036 (Erbudak et al., 1997; Ram, 2001). In addition, the FCC→HCP phase transition is martensitic, resulting in a substantial thermal hysteresis between the heating and cooling transformations and a considerable change in the stacking sequence.

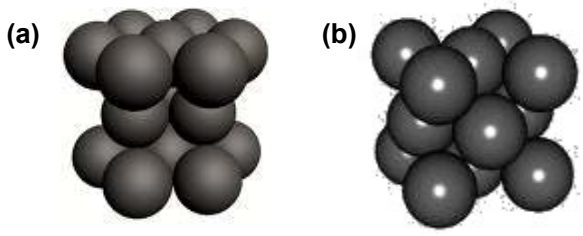

Fig. 2.1 Representations of the (a) HCP and (b) FCC crystal structures of Co (Callister; 2000)

Table 2.1 Lattice Parameters, Lattice Surface Area (A), Lattice Volume (V), and Calculated Densities (ρ) for HCP-Co, FCC-Co, and ε-Co (ICDD Card No. 5-0727 and 15-0806; Dinega and Bawendi, 1991; Sun and Murray, 1999; Ram, 2001)

Crystal Structure	Lattice Parameters, nm	A, 10^{-2} nm^2	V, 10^{-3} nm^3	ρ, g cm^{-3}
HCP	a = 0.2507 c = 0.4070	93.90	66.50	8.836
FCC	a = 0.3545	75.40	44.55	8.788
ε	a = 0.6097	37.17	22.66	8.635

Though thermodynamics predicts that HCP-Co is the stable phase at room temperatures, both phases can co-exists at ambient temperature in bulk samples. Furthermore, studies on Co produced by high-temperature crystallization often yielded mixed phases in one sample, presumably due to the low activation energy of formation of stacking faults for both HCP and FCC-Co (Dinega and Bawendi, 1999; Sun and Murray, 1999).

In the case of fine Co particles, recent works on the preparation of Co nanoparticles by low temperature solution chemistry have similarly produced mixtures of HCP and FCC-Co, with FCC as the predominant phase as indicated by the highest peak in the x-ray diffractograms and supported by the electron diffraction patterns (Toneguzzo et al., 2000; Guo et al., 2002). Additionally, it was then found that FCC-Co has become more stable at ambient conditions when the particle size is reduced. Ram (2001) explained this as the influence of the lower total surface energy of FCC-Co over the HCP phase. From his works, he established that the crystal structure of Co nanoparticles has a direct correlation with their size, and due to the lower surface energy and the consequent lower enthalpy of formation of FCC-Co than HCP-Co, Co nanoparticles are most likely to assume the FCC crystal structure under conditions of equilibrium to minimize their internal energy. Hence, he stipulated that within the size range of 10 – 20 nm, the FCC phase is stable at temperatures below 700 ˚C.

However, there were also evidences that suggest that the stability of FCC-Co at low temperatures is not solely due to particle size (Sato et al., 1997; Kodama, 1999). In support of this, Sato et al. (1997) annealed large Co nanoparticles of about 200 nm in size above the HCP→FCC transition temperature. Nonetheless, slow cooling of the annealed nanoparticles did not convert them to HCP-Co, but resulted to the formation of pure FCC-Co. Lattice defects such as stacking faults, dislocations, and surface oxidation were identified as possible factors that affect the crystal structure of Co nanoparticles (Sato et al., 1997; Ram, 2001; Kodama, 1999). However, Sato et al. (1997) did not explain in detail on how the effects were like. Then again, a more intensive in-situ structural study is needed in order to

qualitatively understand the HCP→FCC phase transformation in Co nanoparticles and its difference from the bulk phase transition.

Increasing development in the field of solution-phase chemical synthesis of Co nanoparticles has led to the discovery of a new phase, albeit metastable, in Co nanoparticles. This phase, designated by Dinega and Bawendi (1999) as epsilon-Co (ε-Co), has a complex cubic primitive structure, belonging to the $P4_132$ space group with a unit cell parameter a = 0.6097 ± 0.0001 nm (Dinega and Bawendi, 1999; Sun and Murray, 1999). Additionally, ε-Co as shown in Fig. 2.2 has 20 Co atoms which are grouped into two types: (a) 12 Type I atoms and (b) 8 Type II atoms that differ only in their local coordination in the lattice.

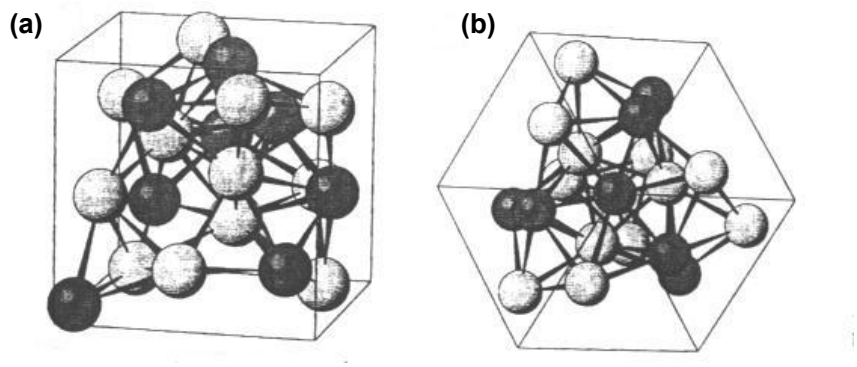

Fig. 2.2 Unit cell of ε-cobalt: (a) unit cell cube filled with eight atoms of Type I (dark) and twelve atoms of Type II (light); (b) the 111-projection of the same cube showing three-fold symmetry along its main diagonal (Dinega and Bawendi, 1999).

Moreover, the ε-Co crystal structure is related to the β-Manganese (β-Mn) structure, a high-temperature phase of Mn stable between 727 – 1095 ˚C, that also has 20 atoms and a lattice parameter of 0.63 nm (Sun and Murray, 1999). Table 2.2 gives the diffraction comparison of the β phase of Mn and the 11 nm Co nanocrystals produced by Sun and Murray (1999) via the reduction of $CoCl_2$

contained in dioctylether solution using superhydride ($LiBEt_3H$) in the presence of oleic acid (OA) and trialkylphosphine (PR_3).

Table 2.2 Comparison of Diffraction Peaks and Relative Intensities of 11 nm Co Nanocrystals and β-Mn (Sun and Murray, 1999)

d_{Co}, *Å*	Rel. Intenstiy	$d_{\beta\text{-}Mn}$, *Å*	Rel. Intenstiy	hkl
2.73	5	2.823	5	210
2.49	4	2.577	5	211
2.16	8	2.231	7	220
2.04	100	2.104	100	221
1.94	56	1.997	60	310
1.85	31	1.904	25	311
1.63	9	1.6872	9	321
1.44	7	1.4874	6	330
1.37	7	1.4115	5	420
1.20	23	1.2377	25	510
1.13	18	1.1721	20	520

Formation of ε-Co is only possible by solution-phase chemistry, particularly by organometallic route, and generally, using a combination of 2 or more tight binding ligands or surfactants like OA, PR_3, triphenylphosphine ($(ph)_3P$), and trioctylphosphane oxide (TOPO) (Dinega and Bawendi, 1999). Organometallic processes, being not thermodynamically controlled, allowed the preparation of metastable structures like ε-Co (Dinega and Bawendi, 1999; Puntes et al., 2002; Shukla et al., 2006; Yang et al., 2006; Cheng and Hight Walker, 2007). On the other hand, the role of these coordinating ligands in the preparation of ε-Co was explained by Dinega and Bawendi (1999) as responsible for changing the energetics of the crystal growth by binding tightly around the growing crystal and around the dissolved Co atoms. In their study, fabrication of Co nanoparticles by thermal decomposition of dicobalt octacarboynyl, $Co_2(CO)_8$, in the absence of TOPO produced exclusive FCC phase.

ε-Co has properties in between the HCP and FCC phases as seen in Table 2.1. Additionally, it is also considered as a soft magnetic material similar to FCC-Co (Dinega and Bawendi, 1999; Sun and Murray, 1999). The magnetic moment per atom and magnetocrystalline anisotropy of ε-Co are compared to the values for bulk HCP-Co and FCC-Co in Table 2.3. The reduced magnetic properties of ε-Co offer several advantages: (a) it facilitates the stabilization of nanoparticles during synthesis, (b) it assists in the particle size classification, and (c) it favors the formation of ordered films for future applications in magnetic recording (Sun and Murray, 1999).

Table 2.3 Magnetic Moment per Atom and Magnetocrystalline Anisotropy of HCP-Co, FCC-Co, and ε-Co (Cullity, 1972; Shukla et al., 2006).

Crystal Structure	Magnetic Moment per Atom, μ_B	Magnetocrystalline Anisotropy, 10^6 erg cm^{-3}
HCP	1.72	4.2
FCC	1.75	2.7
ε	1.70	1.5

μ_B = Bohr Mangeton = 0.927 x 10^{-20} erg/Oe

Phase transition of ε-Co to the HCP or FCC structures can be easily done by annealing at the proper temperature. Heating the sample at 300 ˚C quantitatively converts ε-Co to HCP-Co, while annealing to 500 ˚C completely transforms it to the FCC structure. In addition, subsequent cooling of the heated samples does not revert them back to the original ε-Co structure (Petit et al., 2007).

2.3 Formation of Monosized and Uniformly Dispersed Cobalt and Other Metal Nanoparticles

Preparation of monosized and uniformly dispersed metal nanoparticles is very challenging because of the strong tendency of the nanoparticles to agglomerate

in order to reduce their high surface energy (Sugimoto, 2001; Cao, 2004). These attractive forces, a combination of Brownian motion and attractive van der Waals forces in nanoparticles, are even greater for Co nanoparticles due to the added influence of their magnetic property (Yondong, 2003). Thus, various strategies have been proposed to facilitate the formation of well-dispersed and uniformly sized metal nanoparticles.

Generally, all monodispersed systems, with those having approximately 5% or less in the relative standard deviation of the particle size distribution, fulfill the following conditions: (a) the separation of nucleation and growth stages during synthesis; (b) if possible, the control of the growth mode; (c) the prevention of random agglomeration of growing particles; and (d) the reserve of monomers (Sugimoto, 2001; Cao, 2004).

2.3.1 Separation of Nucleation and Growth

This condition is critical in ensuring that all nuclei are formed during the nucleation stage and that no further nucleation happens during the subsequent growth, such that all preformed nuclei will grow at the same time leading to the formation of monosized nanoparticles (Sugimoto, 2001; Cao, 2004; Cushing et al., 2004; Burda et al., 2005). This requirement was first expressed by La Mer and co-workers in their study on sulfur sols in the 1950s (Viau et al., 1996; Watzky and Finke, 1997; Yondong, 2003). Their proposed mechanism on the formation of monodispersed colloidal particles in homogeneous solutions is the widely cited La Mer mechanism.

According to the La Mer model, formation of colloidal particles is achieved by nucleation from a supersaturated homogenous solution followed by the diffusive growth either by molecular addition or by agglomeration to other solid particles (Watzky and Finke, 1997; Dong et al., 2001; Yondong, 2003; Burda et al., 2005). The condition of supersaturation is necessary since the energy barrier to nucleation can only be surmounted in supersaturated solutions, where the probability of molecular encounters like those needed for the stepwise sequence of molecular addition is sufficiently high (Watzky and Finke, 1997).

Fig. 2.3 is the La Mer diagram for the formation of monodispersed colloidal particles by homogenous nucleation and growth. During the prenucleation period (Stage I), the concentration of the metal (solute) in the solution increases and reaches the saturation concentration, which corresponds to the equilibrium solubility of the solute in the particular solvent. However, nucleation does not take place until the metal concentration attains the critical supersaturation value (Stage II) above the equilibrium solubility. This critical value represents the activation energy for spontaneous nucleation. After the initial nucleation, the solute concentration drops below the critical supersaturation level (Stage III) and nucleation stops. At the same time, particle growth proceeds until the metal concentration is again equal to the equilibrium solubility. Therefore, nucleation and growth are separated producing uniformly sized colloidal particles. Obviously, a very fast nucleation rate is desirable for a complete separation of nucleation from the growth stage in order to generate monodispersed metal particles.

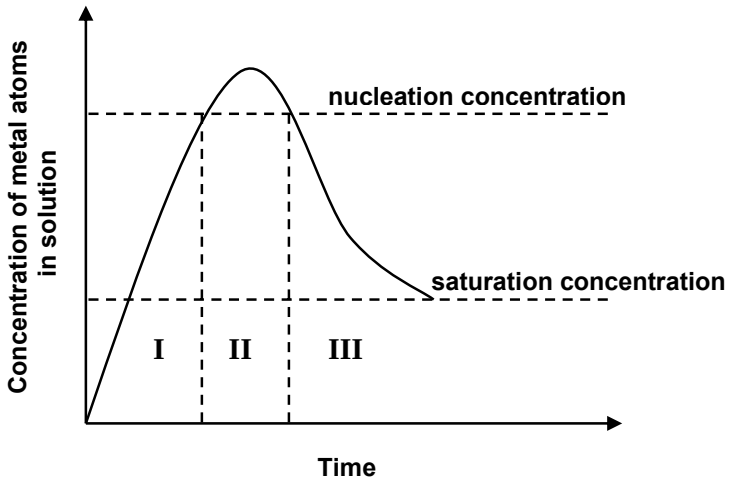

Fig. 2.3 La Mer model for the formation of monodispersed systems by controlled homogenous nucleation and growth: I. prenucleation period; II. nucleation step; III. growth step (Redrawn from Viau et al., 1996).

In practice, automatic separation of nucleation and growth is difficult to accomplish and thus, the solute concentration is normally brought abruptly to a very high supersaturation and quickly decreased below the critical supersaturation level so that a sharp nucleation is achieved (Cao, 2004). Such techniques are called supersaturation quenching. Examples of these processes are reduction of pH in the forced hydrolysis of metal ions, dilution with the solvent, addition of some growth accelerators, and a quick change of temperature (Sugimoto, 2001).

The La Mer model for the separation of nucleation and growth has been widely applied in various syntheses of monodispersed particles in homogeneous solutions. However, inconsistencies were found in some cases, such as in the formation of gold sols, where kinetics was found to play a part, which does not agree with the supersaturation theory (Watzky and Finke, 1997). A more recent mechanism was proposed by Watzky and Finke (1997) to account for the role of kinetics in the separation of nucleation and growth. Their works on iridium nanocluster formation using hydrogen gas as reductant demonstrated that (a)

nucleation in a solution is accomplished via low-level continuous slow process in a solution that is far from being saturated and (b) a subsequent autocatalytic surface-growth step achieves the key separation in time necessary for the synthesis monodispersed nanoclusters. Furthermore, in contrast to the La Mer mechanism, the autocatalytic surface growth process is generally not diffusion-limited. Instead, the rate determining step is the metal incorporation onto the particle surface, which in turn is dependent on the surface area. Nonetheless, even with the existence of this new mechanism, the short nucleation time model of La Mer is still more commonly used to explain the precipitation process for many chemical reactions, including the formation of monosized nanoparticles from solution.

A more drastic measure to separate growth from nucleation is by seeding, first used by Zsigmondy for Au colloids (Sugimoto, 2001). In this process, seed crystals are introduced into a monomer solution under a relatively low supersaturation below the critical supersaturation level. Thus, nucleation process is performed in a completely separate system. This route, known as the seed mediated-method, has also been used to synthesize monometallic and bimetallic (core-shell) nanoparticles (Qian and Yang, 2005).

A variation of this process was employed by Viau et al. (2001) in the preparation of CoNi nanopowders in polyol. Very fine nanoparticles of Pd, Pt, or Ag were formed in situ by the introduction of their salts into the metal solution. Since reduction of noble metals occurs first, Co and Ni atoms preferentially deposit on the surface of noble metal nanoparticles resulting to uniformly sized CoNi nanoparticles. Fig 2.4 (a) shows a TEM image of their $Co_{50}Ni_{50}$ nanoparticles seeded

with Pt, while its x-ray diffraction pattern is in Fig. 2.4 (b). Note that no peak related to Pt was identified from the x-ray diffractogram indicating that all Pt nanoparticles were covered by Co and Ni. A more recent work on the use of heterogeneous nucleation employing Ag and Pt as nucleating agents on the formation of $Co_{80}Ni_{20}$ nanoparticles was published by Luna et al. (2004).

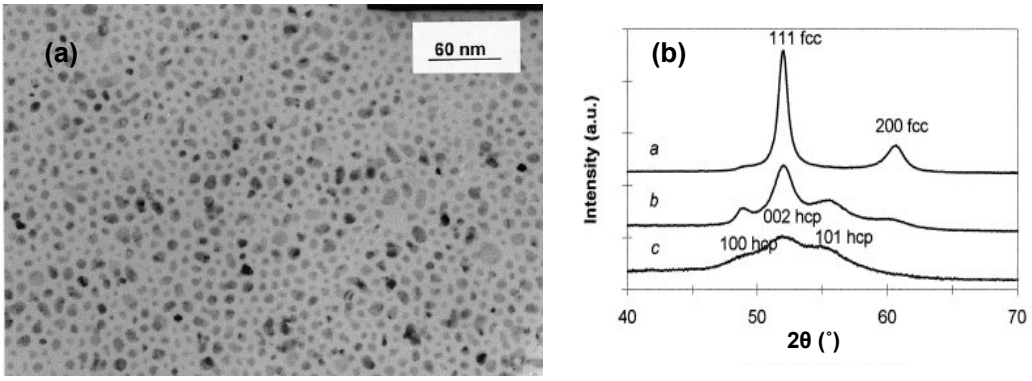

Fig. 2.4 (a) TEM image of $Co_{50}Ni_{50}$ nanoparticles produced by heterogeneous nucleation with Pt in polyol (d_m = 6 nm) and its corresponding (b) XRD pattern with increasing mole ratios of Pt to (Co+Ni) showing only peaks of Co and Ni: a. d_m = 44 nm; b. d_m = 15 nm; c. d_m = 5 nm (Viau et al., 2001).

2.3.2 Control of the Growth Process

Control of growth mode is important in the synthesis of monodispersed nanoparticles since the size distribution of the particles is influenced by the subsequent growth process. Moreover, the final particle size will also be determined by the growth step. Nanoparticles, in general, grow by molecular addition through the stepwise addition of monomeric entities of the solute or by secondary growth process, wherein agglomeration of primary particles occur which form larger secondary particles. (Viau et al., 1996; Yondong, 2003; Burda et al., 2005).

Particle growth via molecular addition involves four major steps: (a) generation of growth species, (b) diffusion of growth species from bulk to the

growth surface, (c) adsorption of the growth species onto the growth surface, and (d) surface growth through irreversible incorporation of the growth species onto the solid surface (Cao, 2004). The first three steps are diffusion-limited processes, whereas the last step is a surface-controlled process (Cao, 2004). Therefore, the particle growth mechanism depends on which among these steps is rate limiting, either a diffusion-controlled or surface-reaction controlled process.

In a diffusion-limited growth, self sharpening of the size distribution is expected to occur as long as the supersaturation is high, though less than the critical supersaturation level to avoid renucleation during particle growth (Sugimoto, 2001). Fig. 2.5 shows that the radius difference among the nanoparticles decreases with the increase in particle size and with prolonged growth time in a diffusion-controlled growth, which supports the formation of uniformly sized nanoparticles (Cao, 2004). To attain a diffusion-dependent growth, several approaches can be done such as by keeping the amount of the growth species extremely low resulting to very large diffusion distance, by increasing the viscosity of the solution as in the case of ethylene glycol when NaOH is added, and by the introduction of a diffusion barrier such as protective agents like gelatin and PVP (poly vinyl pyrrolidone).

On the other hand, self sharpening of size distribution does not occur in surface-reaction controlled growth and only the relative width of the size distribution against the mean size is narrowed (Sugimoto, 2001). Surface-reaction growth can be further divided into two mechanisms: mononuclear growth and polynuclear growth (Cao, 2004). In mononuclear growth, the growth process proceeds layer by layer, such that the growth species are incorporated onto one layer and continues to

another layer only after the previous layer is completed. The difference in the particle size among the nanoparticles increases with the particle size and growth time as seen in Fig. 2.5. Therefore, mononuclear growth does not promote the formation of monodispersed nanoparticles.

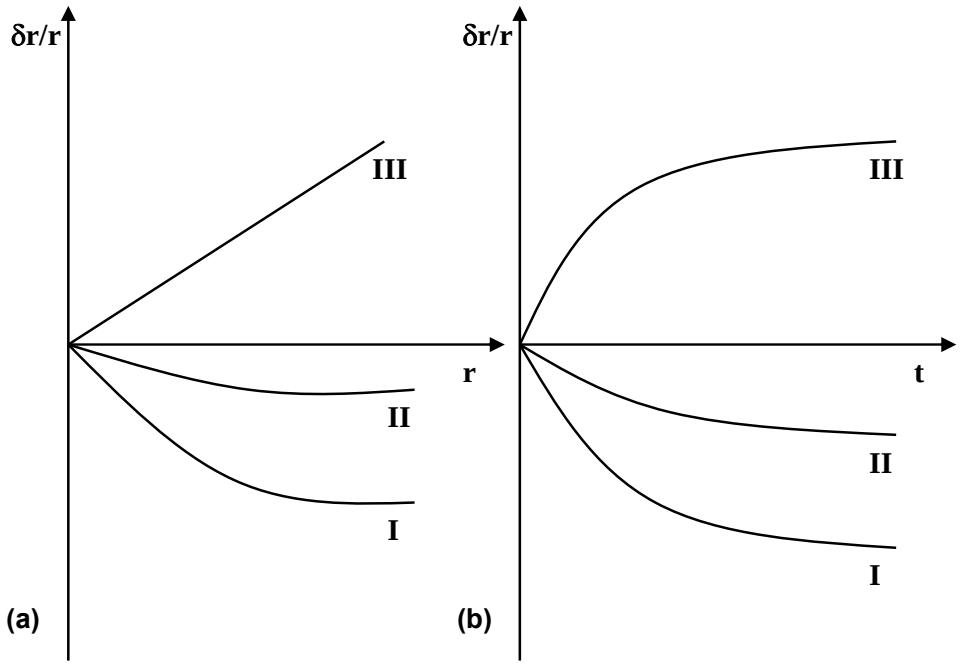

Fig. 2.5 Plot illustrating the radius difference (δr/r) among the nanoparticles as a function of (a) particle radius (r) and (b) growth period (t) for diffusion-controlled growth (I), polynuclear growth (II), and mononuclear growth (III) mechanisms (Modified from Cao, 2004).

However, in polynuclear growth, the surface process is extremely rapid that the second growth layer proceeds before the first layer is completed (Viau, 1996; Cao, 2004). Then, the relative width of the particle size distribution narrows as long as the particle growth continues. From Fig. 2.5, it can be noted that the radius difference among the particles is reduced with the increase in size and with longer growth period. Nonetheless, a predominant diffusion-controlled growth is desirable for the formation of monosized nanoparticles.

In contrast, secondary growth by agglomeration should be avoided since it usually results to a broad size distribution of secondary particles of various shapes. This growth mode also involves diffusion, but in this case, of the primary particles towards a growing cluster of nanoparticles, formed by absorption of the nearest primary particles due to the strong van der Waals forces of large clusters (Sugimoto, 2001). Fig. 2.6 illustrates the model for the nucleation and agglomerative growth in a homogeneous solution (Capek, 2006). It should be noted however that given sufficient time for growth, uniformly sized particles can be produced by agglomeration, though the particles are normally in the submicrometer and micrometer range.

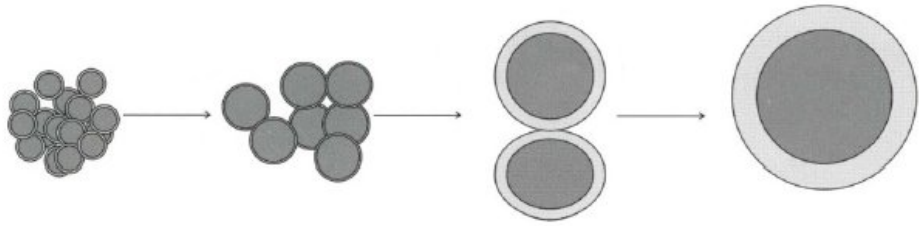

Fig. 2.6 Scheme depicting the growth mechanism by nucleation and agglomeration (Capek, 2006)

2.3.3 Inhibition of Random Agglomeration of Nanoparticles

Besides prevention of secondary growth of nanoparticles, contact between particles during growth stage should be avoided since these contact points serve as active sites for the deposition of the solute (Viau et al., 1996; Sugimoto, 2001; Cao, 2004; Cushing et al., 2004; Burda et al., 2005). Furthermore, once the growth species deposits on preferentially on these contact points, the particles in contact will be permanently cemented together. Common measures for the inhibition of particle agglomeration are by electrostatic repulsion and by steric stabilization.

Electrostatic repulsion makes use of the electric double layer, wherein charged particles exert repulsive forces against each other as function of the zeta potential and Debye length (Sugimoto, 2001; Cao, 2004). These repulsive forces results from the chemisorption of charged species at the surfaces of the nanoparticles. This can be accomplished by diluting the solution or by adjusting the pH. Even so, electrostatic stabilization is limited by the following facts: (a) it is a kinetic type of stabilization, thus, it is almost impossible to re-disperse agglomerated nanoparticles; (b) it is only applicable to dilute systems; (c) it cannot be used on electrolyte sensitive systems; and (d) it is difficult to apply to multiphase systems, since different solids develop varying surface charge and electric potential in a given condition (Cao, 2004).

A more typical measure against particle coagulation is by steric stabilization. It is a widely applied method than electrostatic stabilization due to issues on the stability of nanoparticles at very high or low pH (Burda et al., 2005) when electrostatic stabilization is used and is generally accomplished by the addition of protective agents like polymers, surfactants, and complexing agents, as adsorptive to particles (Sugimoto, 2001). Also, protective agents not only prevent agglomeration, but often act as growth inhibitors and shape controllers as well. Moreover, polymer layer adsorbed on the surface of the nanoparticles also serves as diffusion barrier to growth species resulting in a diffusion-limited growth (Cao, 2004). Table 2.4 gives some of the common protective agents that were used in the synthesis of Co nanoparticles.

Table 2.4 Some Protective Agents Used in the Synthesis of Co Nanoparticles

Protective Agents	References
Trialkylphosphine, PR_3	Sun and Murray, 1999; Yang et al., 2006.
Trioctylphosphane oxide, TOPO	Dinega and Bawendi, 1999; Puntes et al., 2001; Shukla et al., 2006; Cheng and Hight Walker, 2007.
Oleic acid, OA	Sun and Murray, 1999; Viau et al., 2001; Puntes et al., 2002; Luna et al., 2003; Shukla et al, 2006; Yang et al, 2006.
Lauric acid, LA	Luna et al., 2003.
Sodium dodecylsulfosuccinate, SDS	Rivas et al, 1999; Gibot et al., 2005.
Didodecyldimethyl ammonium bromide, DDAB	Chen et al., 1995; Ram, 2001.
Centrimethyl ammonium bromide, CTAB	Gibot et al., 2005
1,2 propanediol	Viau et al., 1994; Toneguzzo et al., 2000; Luna et al., 2004.
1,2 hexadecanediol	Luna et al., 2003.

Alkylphosphines molecules such as PR_3 and TOPO due to their steric bulkiness, in combination with the organic molecules of oleic acid, are generally employed in the preparation of ε-Co by organometallic method. As mentioned, these molecules were found to be responsible for changing the energetics of crystal growth during synthesis in favor of the formation of the less dense ε-Co (Dinega and Bawendi, 1999). In addition, by changing the mole ratio of these protective agents in the solution, anisotropic Co nanoparticles can be produced (Puntes et al., 2001; Shukla et al., 2006). On the other hand, cationic (SDS) and anionic (DDAB and CTAB) surfactants are normally used in microemulsion and metal salt reduction techniques to fabricate either a single phase FCC-Co or a mixture of both phases (Chen et al., 1995; Rivas, 1999). Meanwhile, polyalchohols such as 1,2 propanediol and 1,2 hexadecanediol can act simultaneously as solvent, protective agent, and reductant during the fabrication of monodispersed Co nanoparticles by the polyol

process (Viau et al., 1994; Toneguzzo et al., 2000; Luna et al., 2004). Synthetic routes for the preparation of Co nanoparticles such as organometallic route, microemulsion, metal salt reduction, and polyol method will be described in detail in the succeeding sections.

2.3.4 Reserve of Monomers

In the formation of monodispersed particles, two conflicting requirements are present during growth stage: moderate supersaturation to avoid renucleation and an ample concentration of monomers for particle growth (Cao, 2004). To resolve this, a monomer reservoir, which regulates the release of metal ions, must be built. This is accomplished by introducing complexing agents like EDTA, NTA, and citric acid that shield a large concentration of multivalent metal cations, and thus decreases the supersaturation of free metal ions in the solution (Sugimoto, 2001). In addition to preventing concurrent nucleation during particle growth, complexing agents also inhibits agglomeration of particles during this stage.

2.4 Liquid-Phase Synthesis of Cobalt and Other Magnetic Nanoparticles

Various synthetic routes have been exploited in the preparation of uniformly sized and monodispersed Co nanoparticles. These methods are generally grouped into two: physical and chemical methods. Physical methods make use of high-energy treatment in gaseous and solid states to form magnetic nanoparticles (Gubin et al, 2005). Examples are laser vaporization, arc discharge, chemical vapor deposition, and low-energy beam cluster deposition, which utilize special installations or apparatus during synthesis (Cao, 2004; Burda et al, 2005; Gubin et al., 2005).